

A Time Integration Algorithm for Structural Dynamics With Improved Numerical Dissipation: The Generalized- α Method

J. Chung

Graduate Research Assistant.

G. M. Hulbert

Assistant Professor,
Assoc. Mem. ASME.

Department of Mechanical Engineering,
and Applied Mechanics,
The University of Michigan,
Ann Arbor, MI 48109-2125

A new family of time integration algorithms is presented for solving structural dynamics problems. The new method, denoted as the generalized- α method, possesses numerical dissipation that can be controlled by the user. In particular, it is shown that the generalized- α method achieves high-frequency dissipation while minimizing unwanted low-frequency dissipation. Comparisons are given of the generalized- α method with other numerically dissipative time integration methods; these results highlight the improved performance of the new algorithm. The new algorithm can be easily implemented into programs that already include the Newmark and Hilber-Hughes-Taylor- α time integration methods.

1 Introduction

The need has been long recognized for step-by-step time integration algorithms to possess algorithmic damping when solving structural dynamics problems. In particular, it is desirable to have controllable numerical dissipation in the higher frequency modes since, using standard finite elements to discretize the spatial domain, the spatial resolution of these high-frequency modes typically is poor. By using algorithms with high-frequency dissipation, spurious high-frequency response may be damped out. Also, when solving highly nonlinear problems, high-frequency numerical dissipation has been found to improve the convergence of iterative equation solvers. However, the addition of high-frequency dissipation should not incur a loss of accuracy nor introduce excessive algorithmic damping in the important low frequency modes. For example, the Newmark family of algorithms contains methods that possess high-frequency dissipation (Newmark, 1959); however, these methods are only first-order accurate and are too dissipative in the low-frequency domain. Numerous dissipative algorithms have been developed that attain high-frequency dissipation with little low-frequency damping while maintaining second-order accuracy; e.g., the θ method of Wilson (1968), the HHT- α method of Hilber, Hughes and Taylor (1977), the WBZ- α method of Wood, Bossak, and Zienkiewicz (1981), the ρ method of Bazzi and Anderheggen (1982) and the θ_1 -

method of Hoff and Pahl (1988a, 1988b) (also Hoff et al. (1989)).

The matrix equation of linear structural dynamics is

$$\mathbf{M}\ddot{\mathbf{X}} + \mathbf{C}\dot{\mathbf{X}} + \mathbf{K}\mathbf{X} = \mathbf{F} \quad (1)$$

where \mathbf{M} , \mathbf{C} , and \mathbf{K} are the mass, damping, and stiffness matrices, respectively, \mathbf{F} is the vector of applied loads (a given function of time), \mathbf{X} is the vector of displacement unknowns, and superposed dots indicate differentiation with respect to time. The initial value problem consists of finding a function $\mathbf{X} = \mathbf{X}(t)$ which satisfies (1) for all $t \in [0, t_N]$, $t_N > 0$, and the initial conditions

$$\mathbf{X}(0) = \mathbf{d} \quad (2)$$

$$\dot{\mathbf{X}}(0) = \mathbf{v} \quad (3)$$

where \mathbf{d} and \mathbf{v} are given vectors of initial displacements and velocities, respectively. The numerically dissipative time integration algorithms listed above have the following common form: \mathbf{d}_n , \mathbf{v}_n and \mathbf{a}_n are given approximations to $\mathbf{X}(t_n)$, $\dot{\mathbf{X}}(t_n)$, and $\ddot{\mathbf{X}}(t_n)$, respectively. Expressions for \mathbf{d}_{n+1} and \mathbf{v}_{n+1} are specified as linear combinations of \mathbf{d}_n , \mathbf{v}_n , \mathbf{a}_n and \mathbf{a}_{n+1} . An additional equation is needed to determine \mathbf{a}_{n+1} . This additional equation represents a modified version of Eq. (1). Each algorithm is defined by the specific form of the displacement and velocity update equations and the modified balance equation. Algorithms having this form may be classified as one-step, three-stage (or three-level) time integration methods. The algorithms are one-step methods because the solution at time t_{n+1} depends only on the solution history at time t_n . The three-stage designation refers to the solution being described by the three solution vectors: \mathbf{d}_n , \mathbf{v}_n , and \mathbf{a}_n .

In this paper, we present a new family of one-step, three-stage, numerically dissipative time integration algorithms. This family, which we call the generalized- α method, contains the HHT- α and WBZ- α algorithms; in addition, we identify a new

Contributed by the Applied Mechanics Division of THE AMERICAN SOCIETY OF MECHANICAL ENGINEERS for presentation at the First Joint ASCE-EMD, ASME-AMD, SES Meeting, Charlottesville, VA, June 6-9, 1993.

Discussion on this paper should be addressed to the Technical Editor, Professor Lewis T. Wheeler, Department of Mechanical Engineering, University of Houston, Houston, TX 77204-4792, and will be accepted until four months after final publication of the paper itself in the ASME JOURNAL OF APPLIED MECHANICS.

Manuscript received by the ASME Applied Mechanics Division, Dec. 2, 1991; final revision, Aug. 17, 1992. Associate Technical Editor: C. F. Shih.

Paper No. 93-APM-20.

algorithm that achieves an optimal combination of high-frequency and low-frequency dissipation. That is, for a given value of high-frequency dissipation, this optimal algorithm minimizes the low-frequency dissipation. From a practical viewpoint, the generalized- α method is particularly convenient since the algorithmic parameters are defined in terms of the desired amount of high-frequency dissipation. The design of the generalized- α method is discussed and comparisons with other numerically dissipative algorithms are provided that demonstrate the improved performance of the new time integration method.

2 The Generalized- α Algorithm

The basic form of the generalized- α method is given by

$$\mathbf{d}_{n+1} = \mathbf{d}_n + \Delta t \mathbf{v}_n + \Delta t^2 \left(\left(\frac{1}{2} - \beta \right) \mathbf{a}_n + \beta \mathbf{a}_{n+1} \right) \quad (4)$$

$$\mathbf{v}_{n+1} = \mathbf{v}_n + \Delta t ((1 - \gamma) \mathbf{a}_n + \gamma \mathbf{a}_{n+1}) \quad (5)$$

$$\mathbf{M} \mathbf{a}_{n+1-\alpha_m} + \mathbf{C} \mathbf{v}_{n+1-\alpha_f} + \mathbf{K} \mathbf{d}_{n+1-\alpha_f} = \mathbf{F}(t_{n+1-\alpha_f}) \quad (6)$$

$$\mathbf{d}_0 = \mathbf{d} \quad (7)$$

$$\mathbf{v}_0 = \mathbf{v} \quad (8)$$

$$\mathbf{a}_0 = \mathbf{M}^{-1}(\mathbf{F}(0) - \mathbf{C} \mathbf{v} - \mathbf{K} \mathbf{d}) \quad (9)$$

where

$$\mathbf{d}_{n+1-\alpha_f} = (1 - \alpha_f) \mathbf{d}_{n+1} + \alpha_f \mathbf{d}_n \quad (10)$$

$$\mathbf{v}_{n+1-\alpha_f} = (1 - \alpha_f) \mathbf{v}_{n+1} + \alpha_f \mathbf{v}_n \quad (11)$$

$$\mathbf{a}_{n+1-\alpha_m} = (1 - \alpha_m) \mathbf{a}_{n+1} + \alpha_m \mathbf{a}_n \quad (12)$$

$$t_{n+1-\alpha_f} = (1 - \alpha_f) t_{n+1} + \alpha_f t_n \quad (13)$$

in which $n \in \{0, 1, \dots, N-1\}$, N is the number of time steps and Δt is the time step. The displacement and velocity update Eqs. (4) and (5) are identical to those of the Newmark algorithm. The structure of these update equations was obtained by restricting the sum of the coefficients of their acceleration terms to equal the coefficient of the acceleration term in a Taylor series expansion of $\mathbf{d}(t_{n+1})$ and $\mathbf{v}(t_{n+1})$ about t_n . Simple numerical experiments have shown that this update equation structure results in a monotone increase per period in the peak displacement and velocity errors. The modified balance equation, (6), is effectively a combination of the HHT- α and WBZ- α balance equations. The crucial task is to determine relationships between the algorithmic parameters, α_f , α_m , β , and γ . With appropriate expressions for γ and β , if $\alpha_m = 0$, the algorithm reduces to the HHT- α method; $\alpha_f = 0$ produces the WBZ- α method; $\alpha_m = \alpha_f = 0$ gives rise to the Newmark family. We shall show that other choices of the algorithmic parameters engender time integration algorithms with better numerical dissipation characteristics.

3 Analysis of the Generalized- α Algorithm

For purposes of analysis, it is advantageous to reduce the coupled equations of motion and the algorithmic equations to a series of uncoupled single-degree-of-freedom systems. This is accomplished by invoking the property of eigenvector orthogonality; see, e.g., (Hughes, 1987). The single-degree-of-freedom problem is given by

$$\ddot{u} + 2\zeta\omega\dot{u} + \omega^2 u = f, \quad (14)$$

and $u(0) = d$, $\dot{u}(0) = v$. To study the accuracy and stability properties of an algorithm, it suffices to consider $f = 0$ for all $t \in [0, t_N]$. The generalized- α method, applied to (14) with $f = 0$, may be written in the compact form

$$\mathbf{X}_{n+1} = \mathbf{A} \mathbf{X}_n, \quad n \in \{0, 1, \dots, N-1\} \quad (15)$$

in which $\mathbf{X}_n = \{d_n, \Delta t v_n, \Delta t^2 a_n\}^T$; \mathbf{A} is called the amplification matrix.

The accuracy of an algorithm may be determined from its local truncation error, τ , defined by

$$\tau = \Delta t^{-2} \sum_{i=0}^3 (-1)^i A_i u(t_{n+1-i}) \quad (16)$$

where $A_0 = 1$, A_1 is the trace of \mathbf{A} , A_2 is the sum of the principal minors of \mathbf{A} and A_3 is the determinant of \mathbf{A} . An algorithm is k th order accurate provided that $\tau = O(\Delta t^k)$. The generalized- α method is second-order accurate, provided

$$\gamma = \frac{1}{2} - \alpha_m + \alpha_f. \quad (17)$$

The stability, numerical dissipation and numerical dispersion of an algorithm depend upon the eigenvalues of its amplification matrix. The spectral radius, ρ , of an algorithm is defined by

$$\rho = \max(|\lambda_1|, |\lambda_2|, |\lambda_3|) \quad (18)$$

where λ_i is the i th eigenvalue of \mathbf{A} . Of particular interest is the variation in ρ as a function of $\Omega = \omega \Delta t$. An algorithm is unconditionally stable for linear problems if $\rho \leq 1$ for all $\Omega \in [0, \infty)$ (strictly less than one for repeated real roots). The generalized- α method is unconditionally stable, provided

$$\alpha_m \leq \alpha_f \leq \frac{1}{2}, \quad \beta \geq \frac{1}{4} + \frac{1}{2} (\alpha_f - \alpha_m). \quad (19)$$

The spectral radius also is a measure of numerical dissipation; a smaller spectral radius value corresponds to greater numerical dissipation. Algorithmic damping in the high frequency regime is desired; it should be controllable and should be achieved without inducing excessive dissipation in the important low frequency region. In terms of its spectral radius, an algorithm with these desirable dissipation properties has spectral radius value close to unity in the low-frequency domain and the value smoothly decreases as Ω increases. This smoothness property imposes several restrictions on the values of the amplification matrix eigenvalues.

To discuss these restrictions, we shall order the eigenvalues of \mathbf{A} so that for a convergent algorithm there exists a positive value, e.g., Ω_c , such that if $0 < \Omega < \Omega_c$, then two of the eigenvalues are complex conjugate. These two roots, λ_1 and λ_2 , are the principal roots while λ_3 is the so-called spurious root. Typically, in the low-frequency domain, $|\lambda_3| < |\lambda_{1,2}|$. Thus, for the spectral radius to decrease smoothly as Ω increases, $|\lambda_3| \leq |\lambda_{1,2}|$ for all $\Omega \in [0, \infty)$. Violation of this condition is manifested in the corresponding spectral radius plot as a "cusp" where, as Ω increases, the spectral radius also increases. Such an algorithm possesses more numerical dissipation for values of Ω near the cusp than in the high-frequency region and thus is of less practical interest.

The behavior of the principal roots as a function of Ω is also important. To maximize high-frequency dissipation, the principal roots should remain complex conjugate as Ω increases. If root bifurcation occurs (both principal roots become real), typically one root increases in magnitude with increasing Ω ; this results in a increase in the spectral radius with increasing Ω which corresponds to a decrease in the high-frequency dissipation. High-frequency dissipation is maximized if the principal roots become real in the high-frequency limit. That is, if the principal roots are given by $\lambda_{1,2}(\Omega) = A(\Omega) \pm iB(\Omega)$, where A and B are real numbers and $i = \sqrt{-1}$, then high-frequency dissipation is maximized provided $\lim_{\Omega \rightarrow \infty} B(\Omega) = 0$. For the generalized- α method, this condition is satisfied when

$$\beta = \frac{1}{4} (1 - \alpha_m + \alpha_f)^2. \quad (20)$$

To summarize the smoothness design conditions, we require

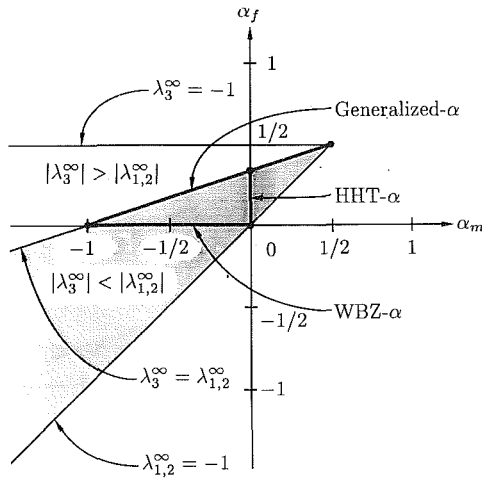


Fig. 1 Classification of generalized- α method in $\alpha_m - \alpha_f$ space

the magnitude of the spurious root to be less than or equal to the magnitude of the principal roots for all Ω and the principal roots to have real values only in the high-frequency limit.

Provided (17), (19), and (20) hold, the generalized- α method can be described in terms of the two remaining free parameters, α_m and α_f ; this is depicted in Fig. 1. The stability region is denoted by the shaded areas; these areas are bounded by two lines: (1) $\lambda_{1,2}^\infty = -1$, which corresponds to $\alpha_m \leq \alpha_f$ in (19); (2) $\lambda_3^\infty = -1$, which corresponds to $\alpha_f \leq 1/2$ in (19); the ∞ superscript on λ_i denotes the high-frequency limit of the root.

Let ρ_∞ denote the user-specified value of the spectral radius in the high-frequency limit (user-specified high-frequency dissipation). Since, by design, we require that $|\lambda_3| \leq |\lambda_{1,2}|$ for all Ω , $\rho_\infty = |\lambda_{1,2}^\infty|$. The value of $\lambda_{1,2}^\infty$ can be obtained using

$$\lambda_{1,2}^\infty = \frac{\alpha_f - \alpha_m - 1}{\alpha_f - \alpha_m + 1}. \quad (21)$$

Thus, given ρ_∞ , we can define α_m and α_f in terms of ρ_∞ . For example, the HHT- α method is given by

$$\alpha_m = 0, \quad \alpha_f = \frac{1 - \rho_\infty}{1 + \rho_\infty} \quad (22)$$

where $\rho_\infty \in [1, 1/2]$. Similarly, using (21) and recalling that $\alpha_f = 0$, the WBZ- α method is given by

$$\alpha_f = 0, \quad \alpha_m = \frac{\rho_\infty - 1}{\rho_\infty + 1} \quad (23)$$

where $\rho_\infty \in [1, 0]$. These are more convenient expressions for the HHT- α and WBZ- α algorithmic parameters than exist in the literature as they directly relate the parameters to the desired value of high-frequency dissipation. We have found that for a given level of high-frequency dissipation, i.e., for fixed ρ_∞ , low-frequency dissipation is minimized when $\lambda_3^\infty = \lambda_{1,2}^\infty$. Using (21) and

$$\lambda_3^\infty = \frac{\alpha_f}{\alpha_f - 1}, \quad (24)$$

low-frequency dissipation is minimized when $\alpha_f = (\alpha_m + 1)/3$. It is more convenient to describe this optimal case by defining α_m and α_f in terms of ρ_∞ :

$$\alpha_m = \frac{2\rho_\infty - 1}{\rho_\infty + 1}, \quad \alpha_f = \frac{\rho_\infty}{\rho_\infty + 1} \quad (25)$$

The generalized- α method, with parametric values given in (17), (20), and (25), is an unconditionally stable, second-order accurate algorithm possessing an optimal combination of high-frequency and low-frequency dissipation.

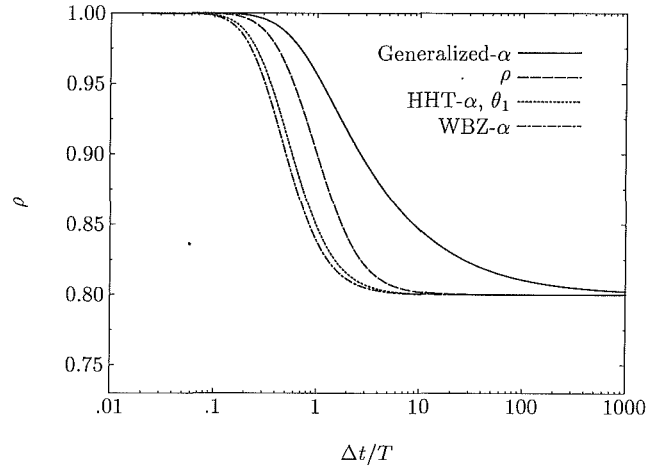


Fig. 2 Comparison of spectral radii of numerically dissipative algorithms

Remarks.

(1) The optimal generalized- α method permits high-frequency dissipation to vary from the no dissipation case ($\rho_\infty = 1$) to the so-called asymptotic annihilation case ($\rho_\infty = 0$). In the latter case, high-frequency response is annihilated after one time step. It is advantageous, from the user viewpoint, to be able to specify the algorithmic parameters in terms of the high-frequency dissipation, ρ_∞ , since the degree of high-frequency dissipation desired is usually a known quantity.

(2) Hoff and Pahl (1988a) presented a generalized algorithm possessing six free parameters; a modified version of this algorithm was developed by Hoff et al. (1989) for consistent treatment of applied loads. The generalized- α method is a member of the modified Hoff-Pahl family (for linear problems) by setting $\hat{\theta}_1 = \hat{\theta}_2 = \hat{\theta}_3 = 1 - \alpha_f$, $\hat{\eta} = (1 - \alpha_m)/(1 - \alpha_f)$, and β and γ given by (20) and (17), respectively. However, we emphasize that the precise definitions of the algorithmic parameters for the optimal case are unique to the present work.

(3) For the optimal case, the spurious root value in the low-frequency limit ($\lambda_3^0 = \lim_{\Omega \rightarrow 0} \lambda_3$) is nonzero. While concern has been expressed in the literature regarding nonzero values of λ_3^0 , we have shown that the impact on algorithmic accuracy is negligible (Hulbert, 1991).

(4) The problem of "overshoot" in displacements obtained by time integration algorithms was studied by Hilber and Hughes (1978). We note that the generalized- α method does not exhibit the overshoot phenomenon.

4 Comparison of Algorithms

In this section, we compare algorithms that possess numerical dissipation, in particular, the HHT- α , WBZ- α , ρ , θ_1 , and generalized- α methods.

Spectral radii of the algorithms are plotted in Fig. 2. For all comparisons, the algorithmic parameters were chosen such that for each algorithm, the spectral radius in the high-frequency limit is 0.8; no physical damping is included in the model problem. It is clear that for the given value of ρ_∞ , the generalized- α method with optimal parameters given by (25) (hereafter referred to as the generalized- α method) has a significantly better spectral radius than the other algorithms. Its improved performance can be seen more clearly when comparing the numerical dissipation and dispersion of the various algorithms.

Measures of numerical dissipation and dispersion are provided by the algorithmic damping ratio and relative period error. Provided the principal roots are complex, these roots may be expressed as

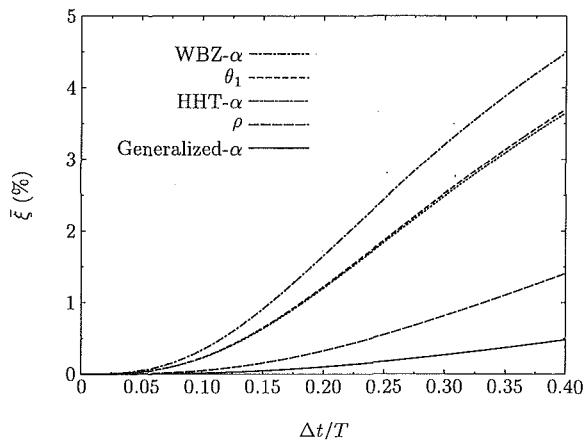


Fig. 3 Algorithmic damping ratios of numerically dissipative algorithms

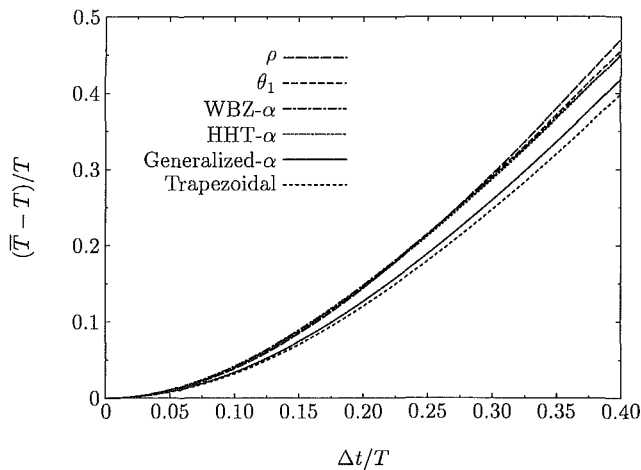


Fig. 4 Relative period errors of time integration algorithms

$$\lambda_{1,2} = \exp(\bar{\omega}\Delta t(-\bar{\xi} \pm i)) \quad (26)$$

where $\bar{\xi}$ and $\bar{\omega}$ are the algorithmic damping ratio and algorithmic frequency, respectively. The relative period error is given by $(\bar{T} - T)/T$, where $T = 2\pi/\omega$ and $\bar{T} = 2\pi/\bar{\omega}$.

Figure 3 shows algorithmic damping ratios for the dissipative algorithms. For the same value of high-frequency dissipation, it can be seen that the generalized- α method has substantially less low-frequency dissipation. Relative period errors are shown in Fig. 4; also included is the relative period error of the trapezoidal rule algorithm. The trapezoidal rule possesses the smallest period error of second-order accurate, unconditionally stable linear multistep methods and thus its period error may be used as a basis to compare the period errors of the numerically dissipative methods. From Fig. 4, it can be seen that the period error of the generalized- α method is closest to that of the trapezoidal rule algorithm.

As a final comparison, (14) was solved using different time integration algorithms with $\omega = \pi$, $\xi = 0$, $d = 1$ and $v = 1$. The displacement error (difference between the exact and numerical displacement values) was computed at $t_N = 0.4$. Figure 5 shows this error as a function of the number of time steps, N , for various algorithms. All algorithms shown achieve second-order accuracy; the ρ -method is not included as it is only first-order accurate. Dahlquist (1963) proved that the trapezoidal rule has the smallest error of unconditionally stable, second-order accurate methods; from Fig. 5 it may be seen that amongst the numerically dissipative algorithms investigated, the generalized- α method has the smallest error.

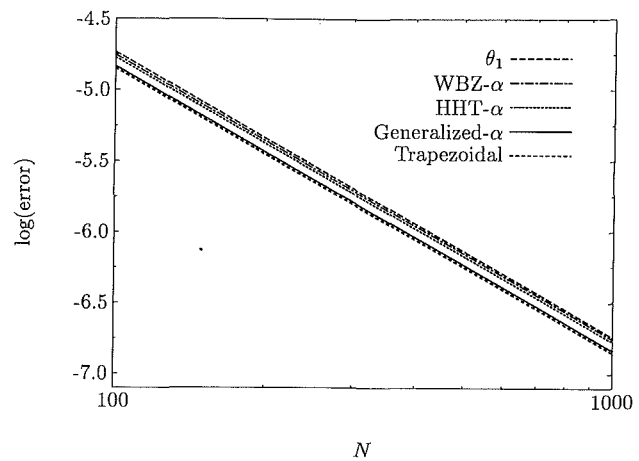


Fig. 5 Comparison of displacement errors of time integration algorithms. N is the number of time steps.

5 Conclusions

A new family of time integration methods has been presented for solving structural dynamics problems. The new scheme includes both the HHT- α and WBZ- α methods; indeed, the new generalized- α method may be considered as a synthesis or generalization of these two methods. An analysis of the generalized- α method was performed to define appropriate values of the algorithmic parameters. Expressions were provided that define the algorithmic parameters in terms of a user-specified value of high-frequency dissipation. The resultant time integration algorithm is unconditionally stable, second-order accurate and possesses an optimal combination of high-frequency and low-frequency dissipation. That is, for a desired level of high-frequency dissipation, the low-frequency dissipation is minimized. The generalized- α method was shown to have better numerical dissipation characteristics, and smaller period and displacement errors than other numerically dissipative schemes. We emphasize that the improved performance of the algorithm is not obtained by increasing the complexity of the algorithm beyond that associated with the HHT- α and WBZ- α methods. This is important from a practical viewpoint since the generalized- α method can be directly implemented with minimal additional coding into programs that already include the Newmark, HHT- α or WBZ- α methods.

The generalized- α method has been presented for structural dynamics. Of interest is extending the method to systems of first-order ordinary differential equations. Research efforts are underway in this area as well as developing improved implicit-explicit time integration methods using the generalized- α method as the parent implicit algorithm.

Acknowledgment

We would like to acknowledge support provided by a Korean Government Overseas Scholarship for the first author.

References

- Bazzi, G., and Anderheggen, E., 1982, "The ρ -Family of Algorithms for Time-Step Integration with Improved Numerical Dissipation," *Earthquake Engineering and Structural Dynamics*, Vol. 10, pp. 537-550.
- Dahlquist, G., 1963, "A Special Stability Problem for Linear Multistep Methods," *BIT*, Vol. 3, pp. 27-43.
- Hilber, H. M., Hughes, T. J. R., and Taylor, R. L., 1977, "Improved Numerical Dissipation for Time Integration Algorithms in Structural Dynamics," *Earthquake Engineering and Structural Dynamics*, Vol. 5, pp. 283-292.
- Hilber, H. M., and Hughes, T. J. R., 1978, "Collocation, Dissipation and 'Overshoot' for Time Integration Schemes in Structural Dynamics," *Earthquake Engineering and Structural Dynamics*, Vol. 6, pp. 99-118.
- Hoff, C., and Pahl, P. J., 1988a, "Development of an Implicit Method with

Numerical Dissipation from a Generalized Single-Step Algorithm for Structural Dynamics," *Computer Methods in Applied Mechanics and Engineering*, Vol. 67, pp. 367-385.

Hoff, C., and Pahl, P. J., 1988b, "Practical Performance of the θ_1 Method and Comparison with Other Dissipative Algorithms in Structural Dynamics," *Computer Methods in Applied Mechanics and Engineering*, Vol. 67, pp. 87-110.

Hoff, C., Hughes, T. J. R., Hulbert, G., and Pahl, P. J., 1989, "Extended Comparison of the Hilbert-Hughes-Taylor α -Method and the θ_1 -Method," *Computer Methods in Applied Mechanics and Engineering*, Vol. 76, pp. 87-93.

Hughes, T. J. R., 1987, *The Finite Element Method: Linear Static and Dynamic Finite Element Analysis*, Prentice-Hall, Englewood Cliffs, New Jersey.

Hulbert, G. M., and Chung, J., 1991, "On the (Non-)Importance of the Spurious Root of Time Integration Algorithms for Structural Dynamics," submitted for publication in *Communications in Applied Numerical Methods*.

Newmark, N. M., 1959, "A Method of Computation for Structural Dynamics," *Journal of the Engineering Mechanics Division ASCE*, Vol. 85, No. EM3, pp. 67-94.

Wilson, E. L., 1968, *A Computer Program for the Dynamic Stress Analysis of Underground Structures*, SESM Report No. 68-1, Division of Structural Engineering and Structural Mechanics, University of California, Berkeley, CA.

Wood, W. L., Bossak, M., and Zienkiewicz, O. C., 1981, "An Alpha Modification of Newmark's Method," *International Journal for Numerical Methods in Engineering*, Vol. 15, pp. 1562-1566.